

Anomalous X-Ray Scattering: Resonant Elastic X-Ray Scattering

T. Egami

*Joint Institute for Neutron Sciences, Department of Materials
Science and Engineering, Department of Physics and Astronomy,
University of Tennessee, Knoxville, TN,
Oak Ridge National Laboratory, Oak Ridge, TN*

Reading:

- ❖ T. Egami and S. J. L. Billinge, *“Underneath the Bragg Peaks: Structural Analysis of Complex Materials”*, Pergamon Materials Series Vol. 7 (Pergamon Press, Elsevier Ltd., Oxford, 2003).
- ❖ Y. Waseda, *“Anomalous X-Ray Scattering for Materials Characterization: Atomic-Scale Structure Determination”* Springer Tracts in Modern Physics 179 (Springer, Berlin, 2002)

Chemical (Compositional) Short-Range Order (CSRO)

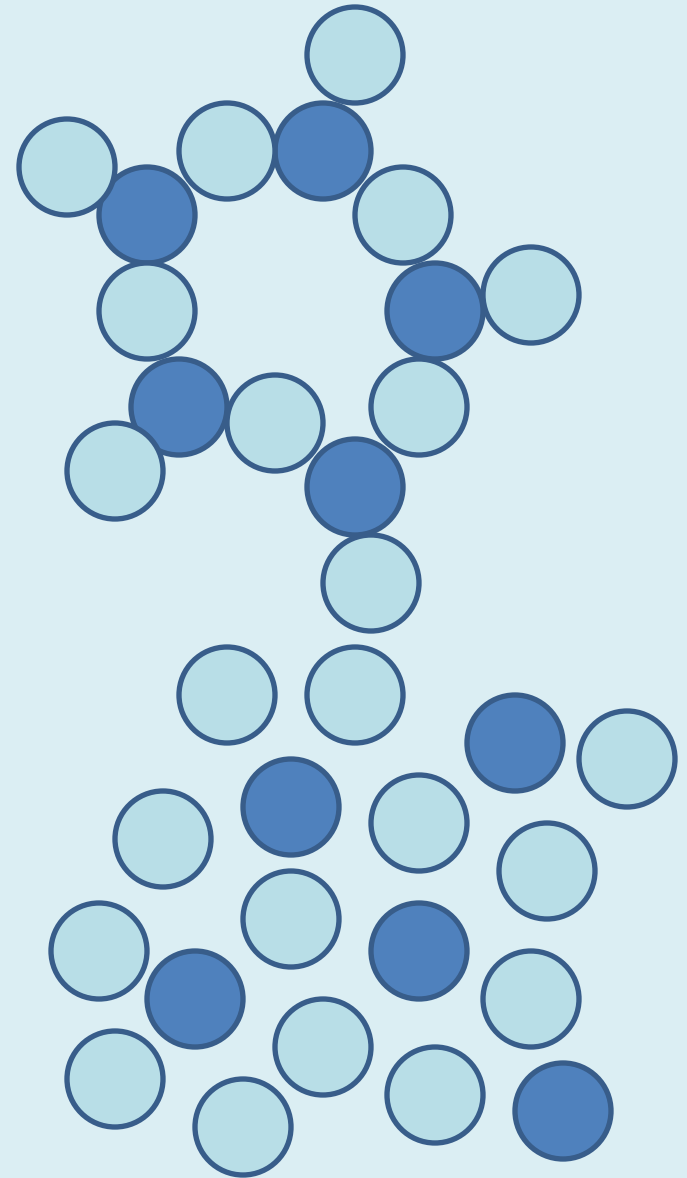
- Well-defined chemical bond (B_2O_3 , SiO_2, \dots).
- Order parameter (Warren)

$$\alpha = 1 - \frac{Z_{AB}}{c_B Z}$$

- Extension by Cargill and Spaepen

$$\eta_{ij} = 1 - \frac{Z_{ij} \langle Z \rangle}{c_j Z_i Z_j}$$

G. S. Cargill, III and F. Spaepen, J. Non-Cryst. Solids **43**, 41 (1981).



Intensity of Elastic X-Ray Scattering

- Structure function, determined from the scattering intensity (see the previous lecture by Prof. Billinge):

$$S(Q) = \frac{1}{\langle f \rangle^2} \sum_{i,j} f_i f_j e^{i\mathbf{Q} \cdot (\mathbf{r}_i - \mathbf{r}_j)}$$

$$S(Q) = \frac{1}{\langle f \rangle^2} \sum_{\alpha,\beta} f_\alpha f_\beta S_{\alpha\beta}(Q), \quad S_{\alpha\beta}(Q) = \sum_{i(\alpha),j(\beta)} e^{i\mathbf{Q} \cdot (\mathbf{r}_i - \mathbf{r}_j)}$$

- Fourier transform:

$$G(r) = \frac{1}{\langle f \rangle^2} \sum_{\alpha,\beta} f_\alpha f_\beta G_{\alpha\beta}(r), \quad G_{\alpha\beta}(r) = \int S_{\alpha\beta}(Q) \sin(Qr) Q dQ$$

$$S_\alpha(Q) = \langle f \rangle \frac{dS(Q)}{df_\alpha} = \frac{1}{\langle f \rangle} \sum_{\alpha,\beta} f_\beta S_{\alpha\beta}(Q),$$

$$G_\alpha(r) = \int [S_\alpha(Q) - 1] \sin(Qr) Q dQ$$

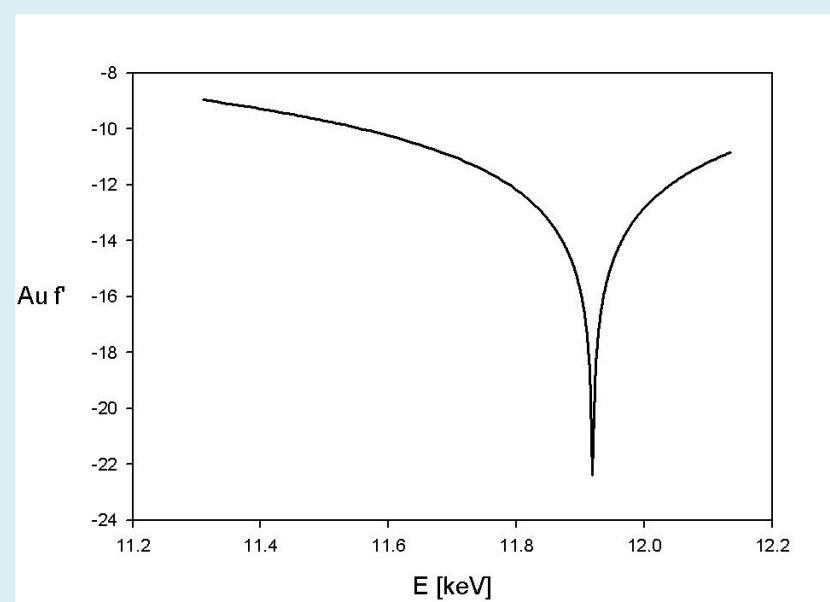
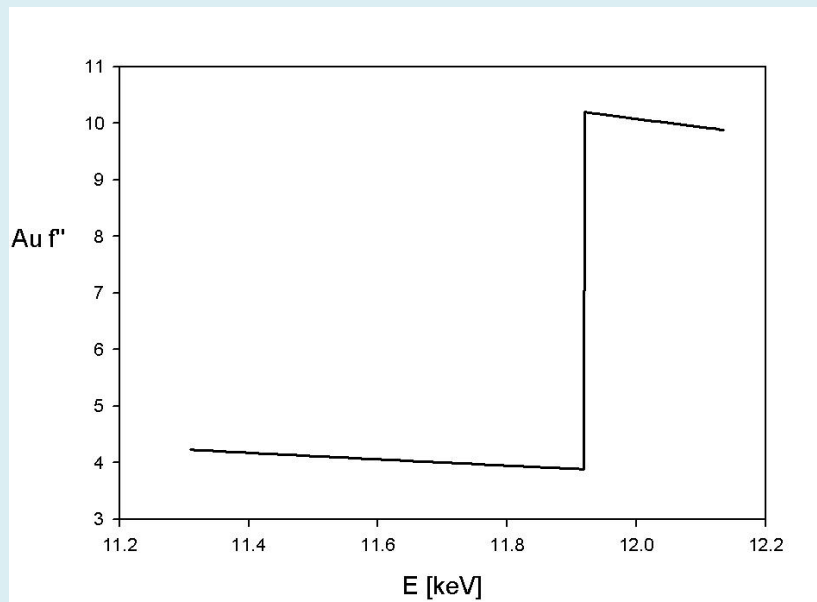
Anomalous X-Ray Scattering:

- Anomalous dispersion:

$$f(Q, E) = f_0(Q) + f'(E) + if''(E), \quad f''(E) \propto \mu(E)$$

- Kramers-Krönich dispersion relation:

$$f'(E) = \frac{2}{\pi} \int_0^{\infty} \frac{f''(E') E'}{E^2 - E'^2} dE'$$



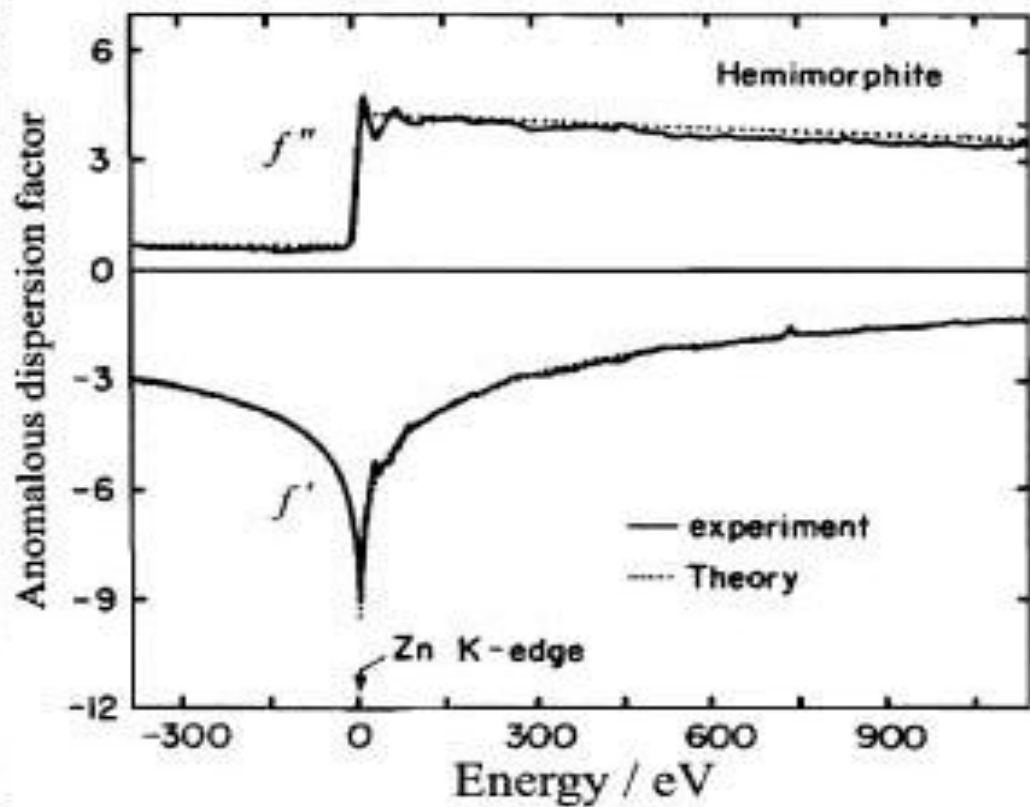


Fig. 4.1. Anomalous dispersion factors of Zn in hemimorphite near the K absorption edge. The values of $f'(E)$ are estimated from the absorption data of $f''(E)$ through the dispersion relation [30]

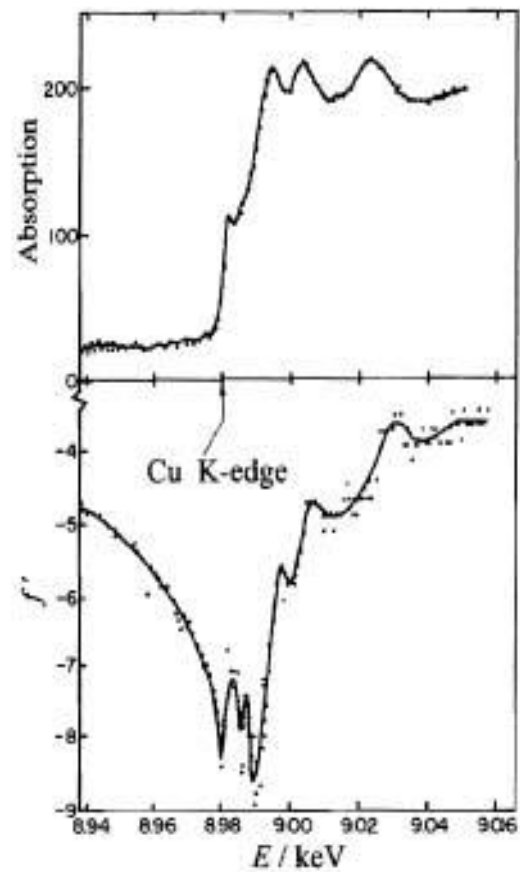
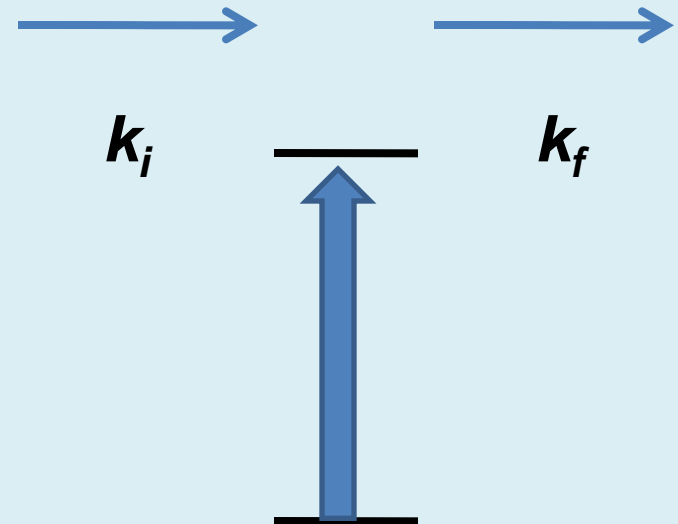


Fig. 4.5. Anomalous dispersion factor f' (bottom) and absorption measured in the energy region near the K absorption edge [39]

X-Ray Resonance

- Incident x-ray induces virtual excitation. Upon de-excitation it emits radiation which interferes with the scattered wave.
- $k_i = k_f$: elastic
- $k_i \neq k_f$: inelastic

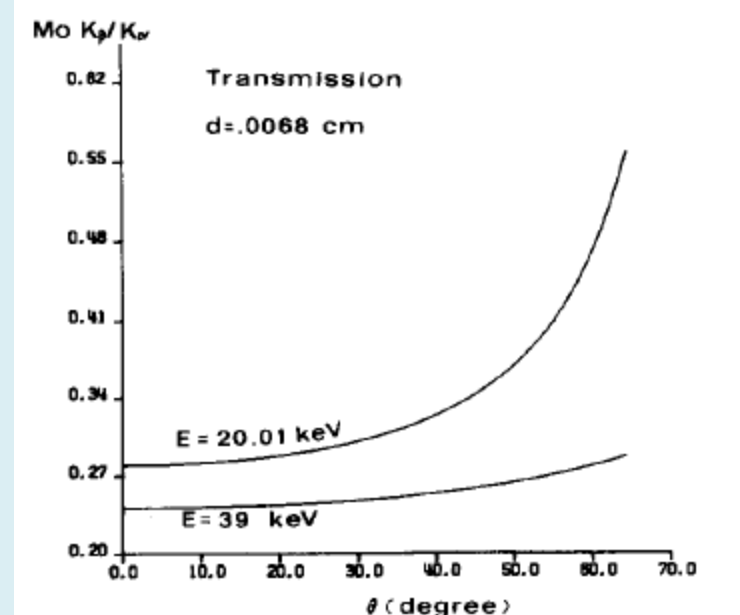
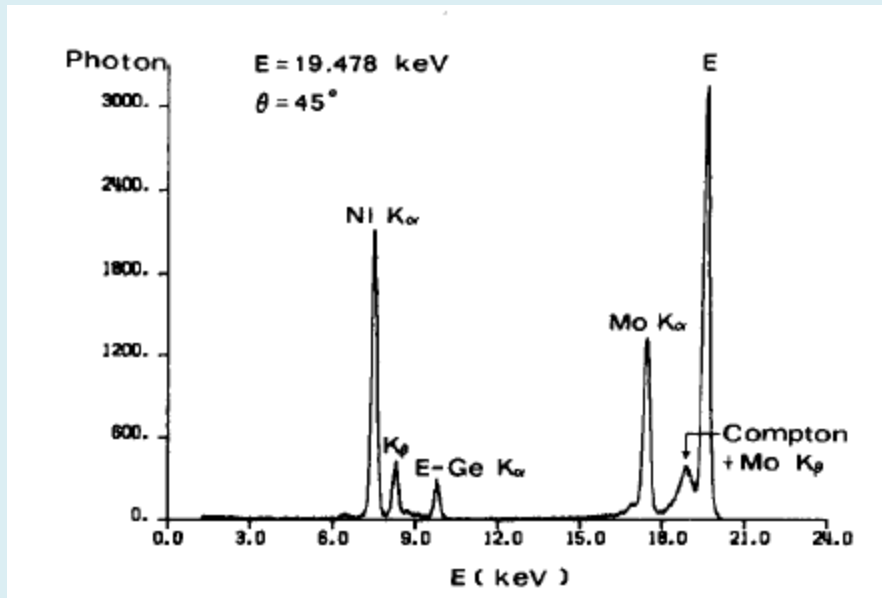


Limitations

- Edge energy: $Q = 2k\sin\vartheta = (2E_j/c\hbar)\sin\vartheta$
- $Q > 15 \text{ \AA}^{-1}$ to obtain good PDF.
- Thus good only for elements heavier than Zr, OK for elements heavier than Ge.
- Excellent for very heavy elements with the reachable L-edge.
- Statistical limitations. Think of combining with neutron scattering.
- But still useful in many occasions.

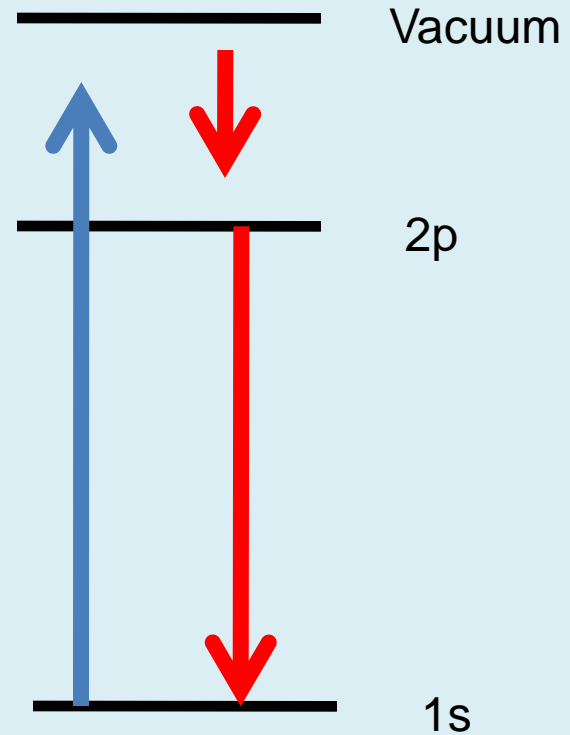
Measurement

- Measure at two energies below the absorption edge.
- X-ray Raman scattering presents a major problem.



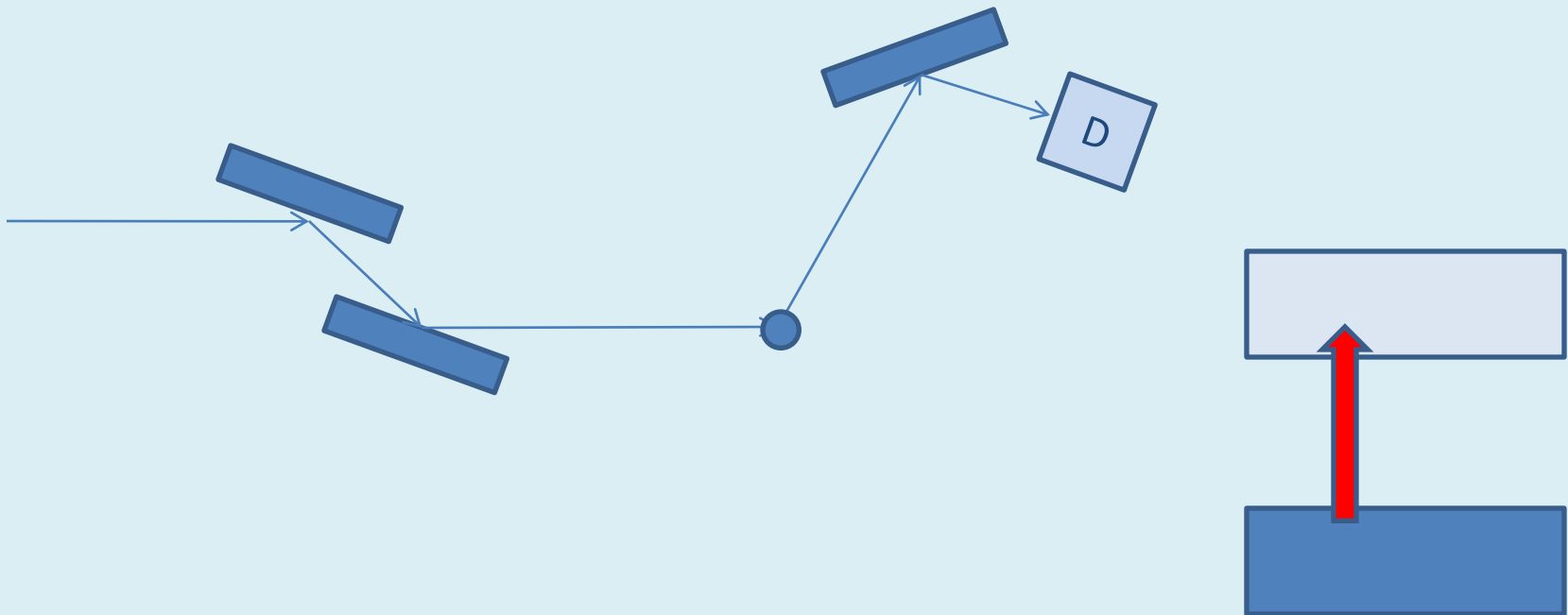
X-Ray Raman

- Characteristic radiation induced by a photon with the energy less than the edge energy, because of the intermediate electronic process involving electron-electron interaction.
- Thus even below the edge you excite some weak fluorescence.



Setup

- Analyzer crystal:
 - Intensity is low, Alignment has to be perfect.
- Energy sensitive semiconductor detector:
 - Intrinsic Ge detector



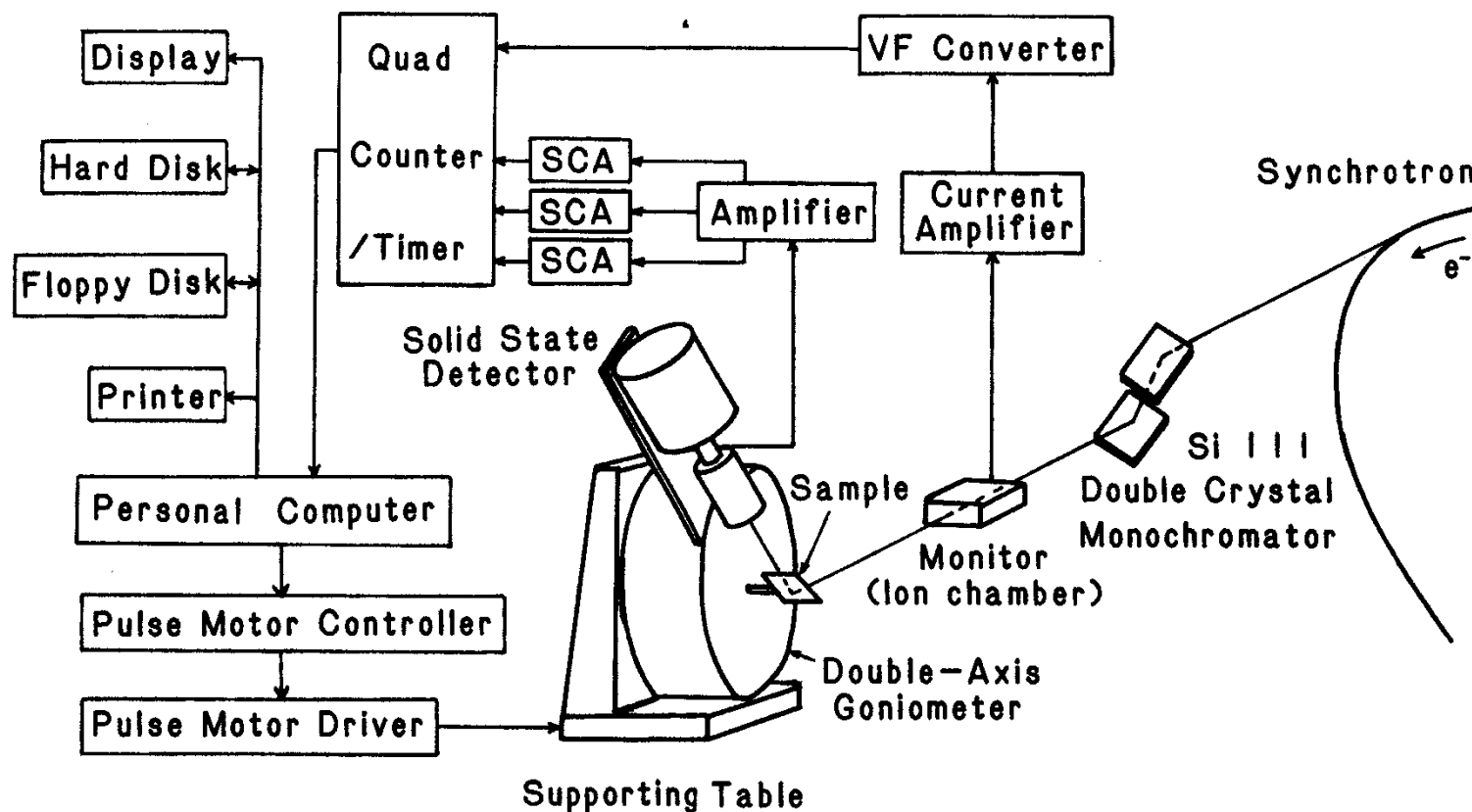


Fig. 5.10. Schematic of the experimental set up including the associated electronics system for the AXS measurements using synchrotron radiation

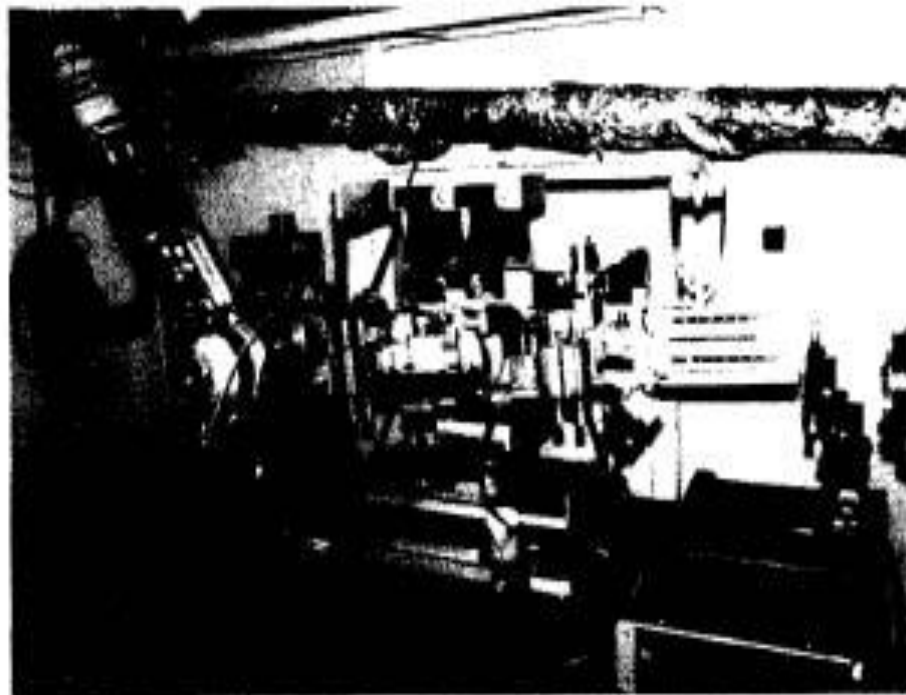
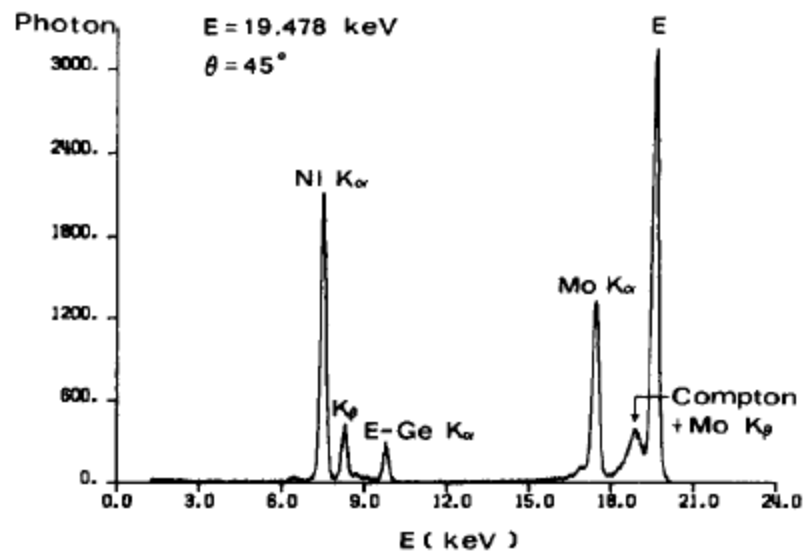
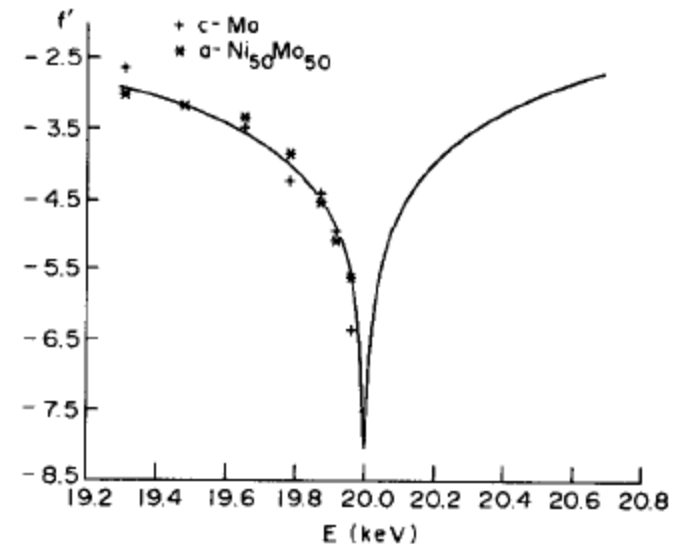
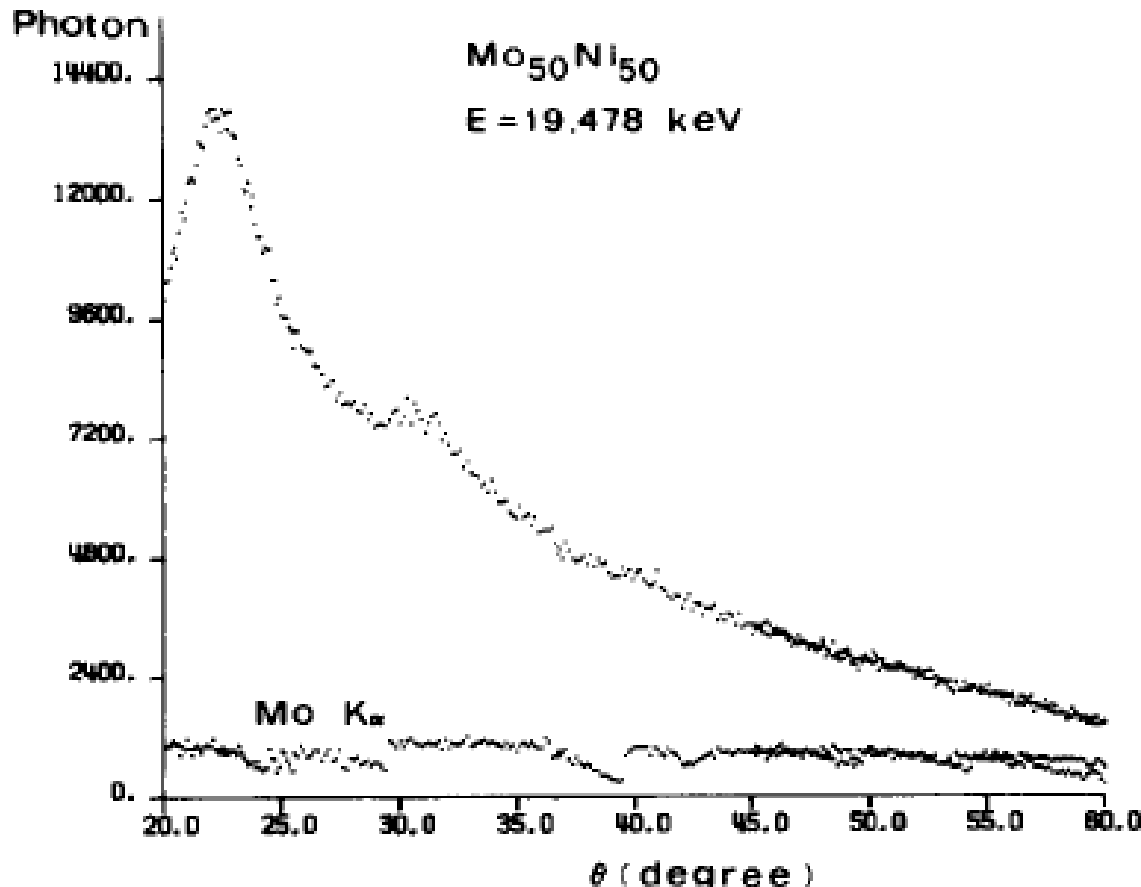


Fig. 5.12. Photograph of the AXS measurements for a liquid sample in the asymmetrical reflection mode with synchrotron radiation [21]

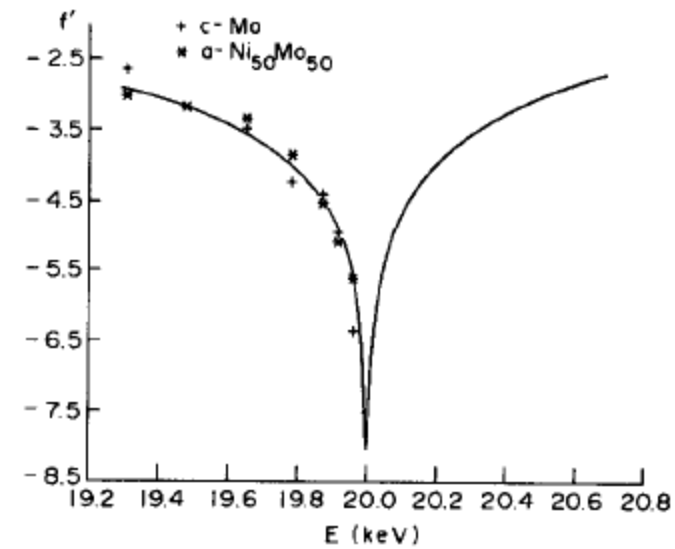
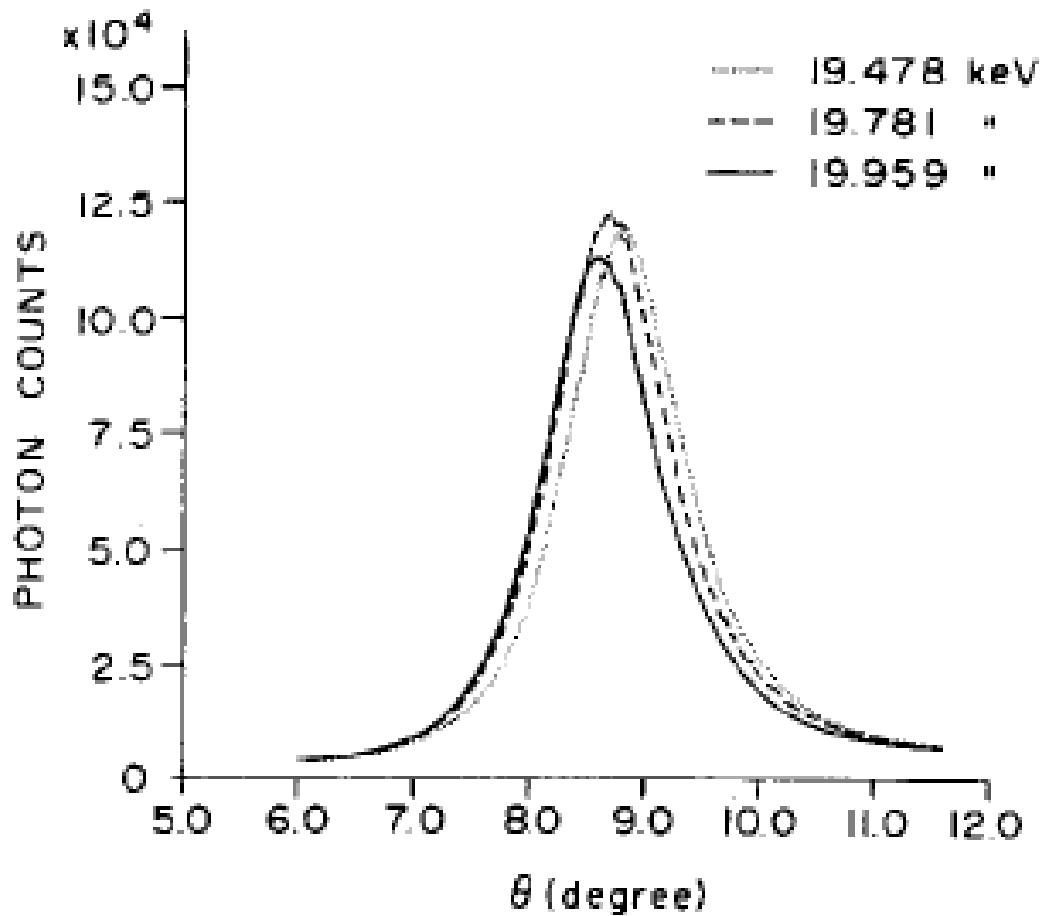


Example

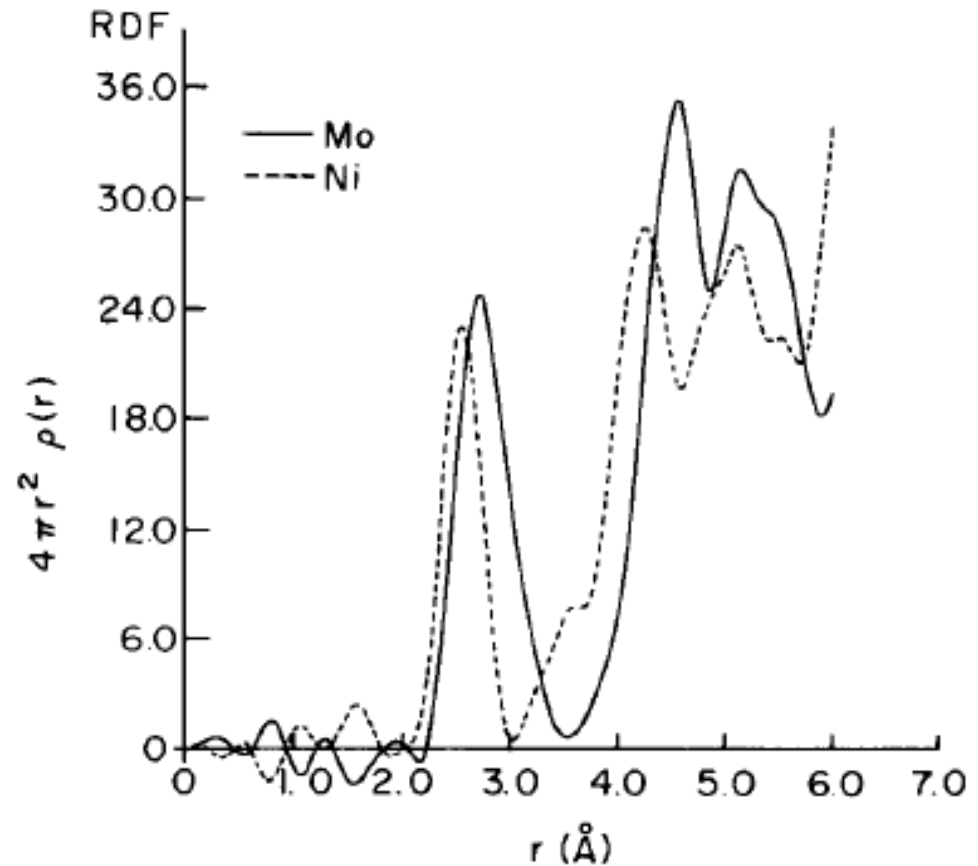
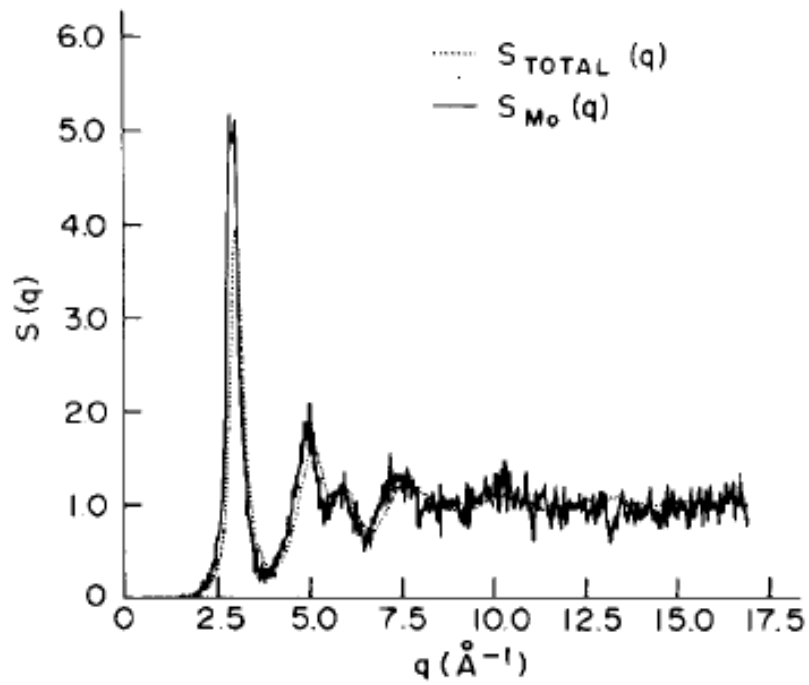


- Higher harmonic component fluctuates with time.

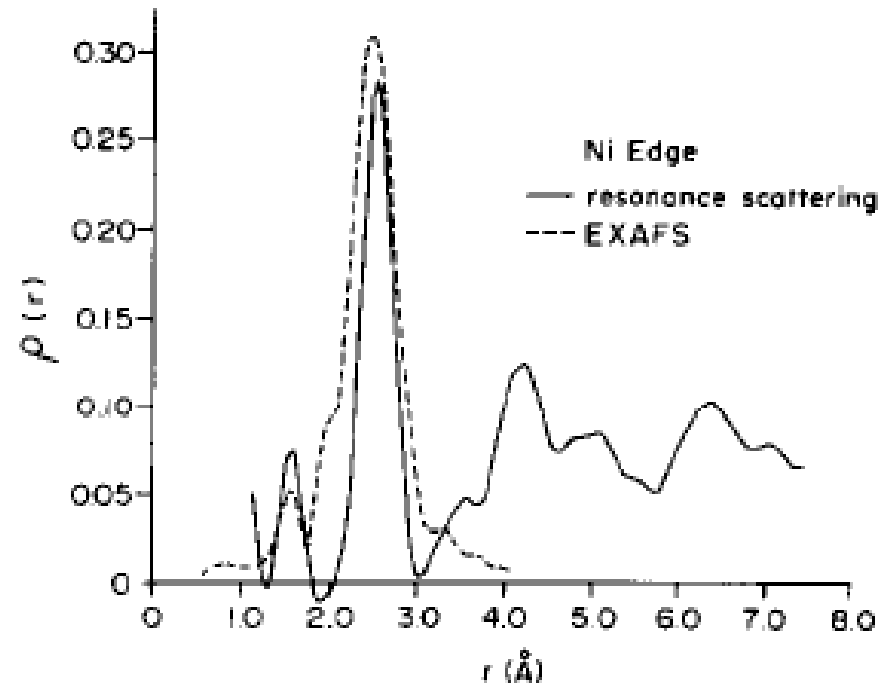
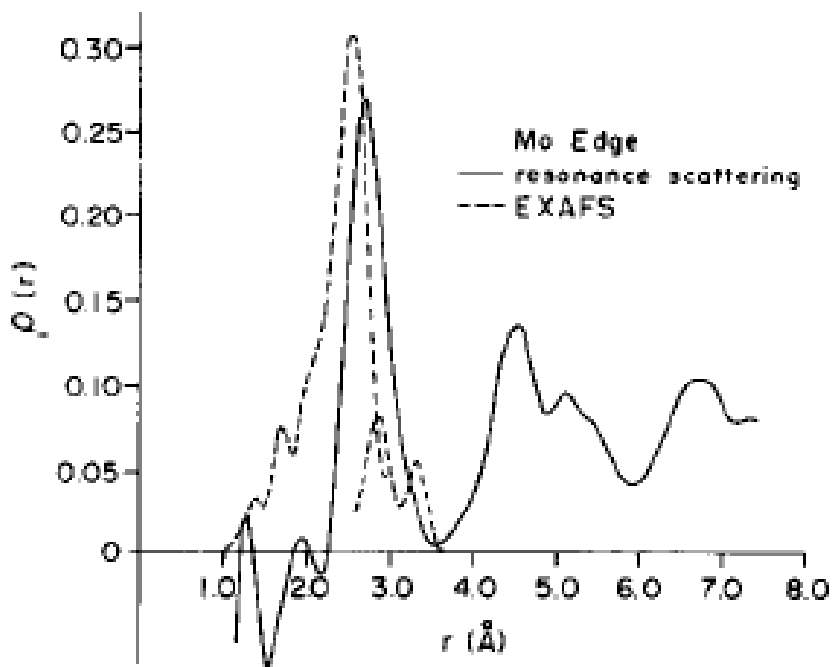
S. Aur, D. Kofalt, Y. Waseda, T. Egami, H.S. Chen, B.K. Teo and R. Wang,
Nucl. Instrum. Methods in Phys. Res. **222**, 259 (1984).



- Differences are small. Requires high accuracy in measurement.



S. Aur, D. Kofalt, Y. Waseda, T. Egami, R. Wang, H.S. Chen, and Boon-Keng Teo, *Solid St. Commun.* **48**, 111 (1983).



- Differential PDF beyond the nearest neighbor.

	First peak position	Coordination number, Z	Integration range to obtain Z
ρ_{total}	2.59 Å		
$4\pi r^2 \rho_{\text{total}}$	2.62	13.4	1.45–3.40 Å
ρ_{Mo}	2.69		
$4\pi r^2 \rho_{\text{Mo}}$	2.72	14.8	2.15–3.55
ρ_{Ni}	2.54	10.0	2.00–3.05
$4\pi r^2 \rho_{\text{Ni}}$	2.57	13.1	2.00–3.70

L-edge

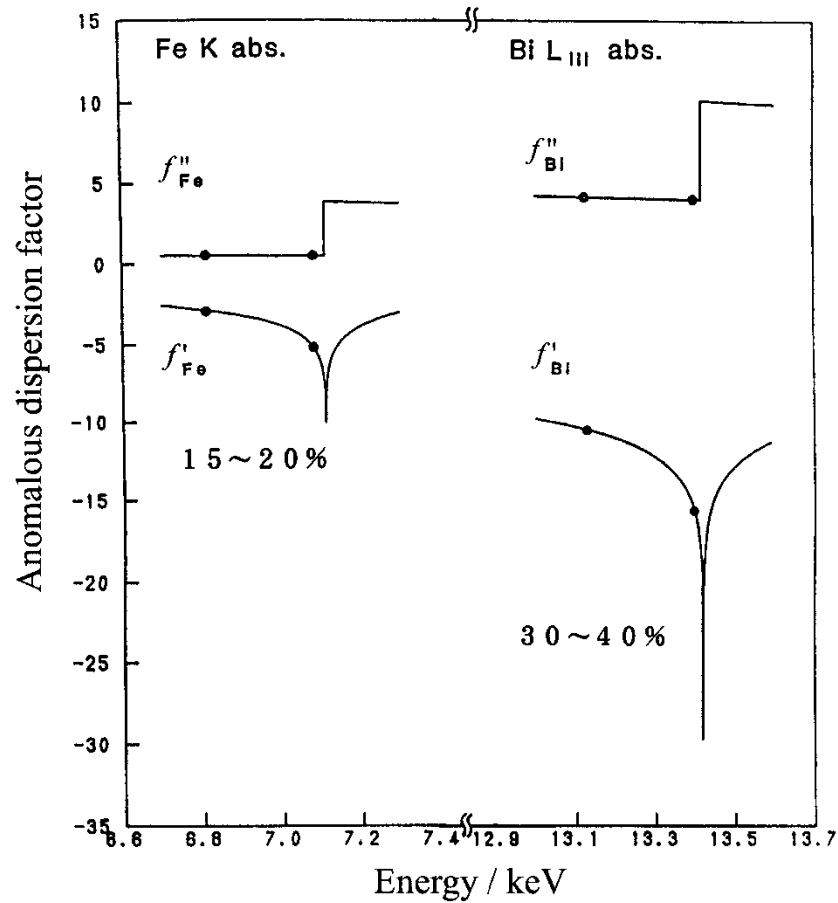
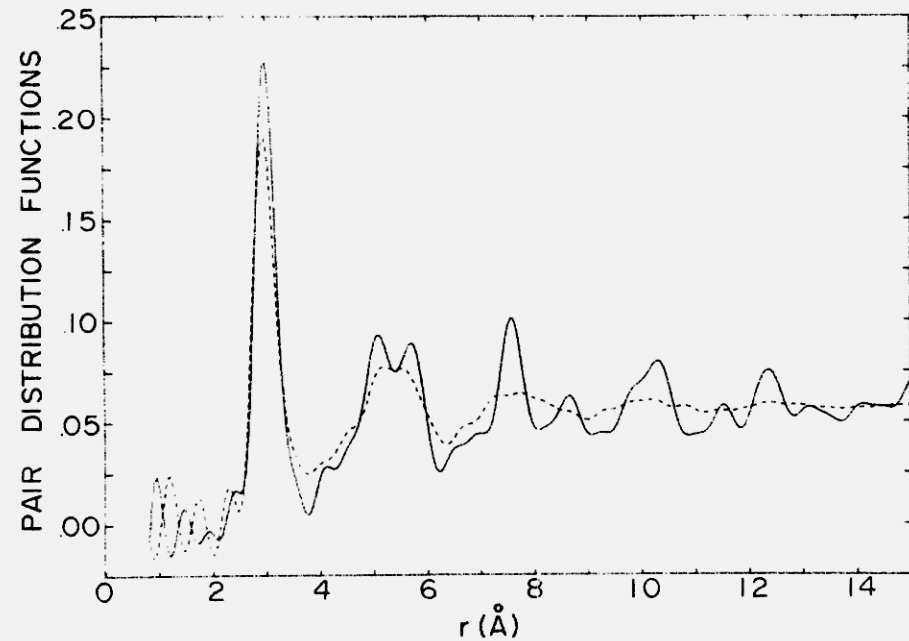
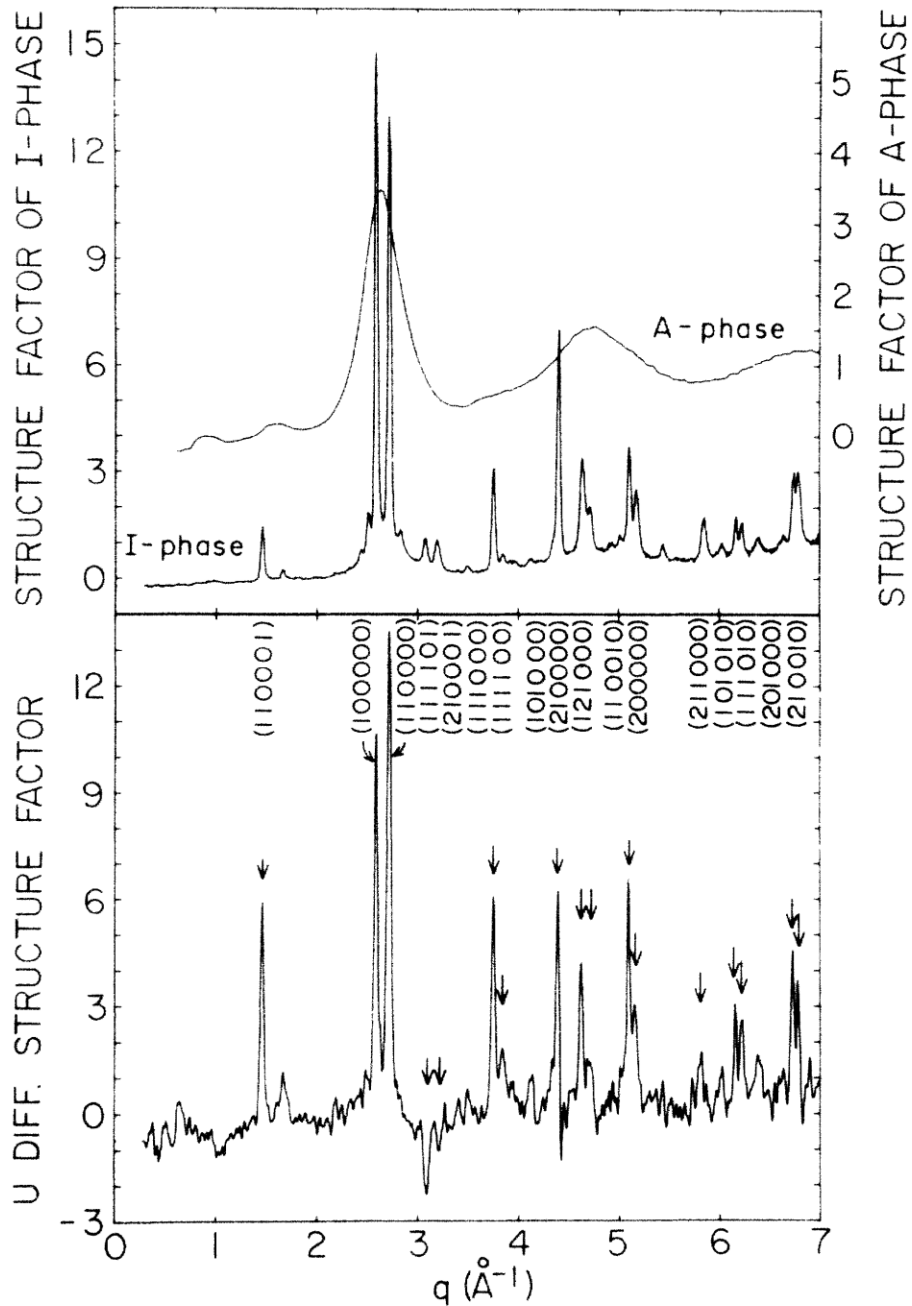


Fig. 10.5. Anomalous dispersion factors of Fe and Bi as a function of energy (calculated values)



Glassy and quasicrystalline Pd-U-Si
 U-L-edge AXS.
 D.D. Kofalt, S. Nano, T. Egami, K.M.
 Wong and S.J. Poon, *Phys. Rev. Lett.*
57, 114 (1986)

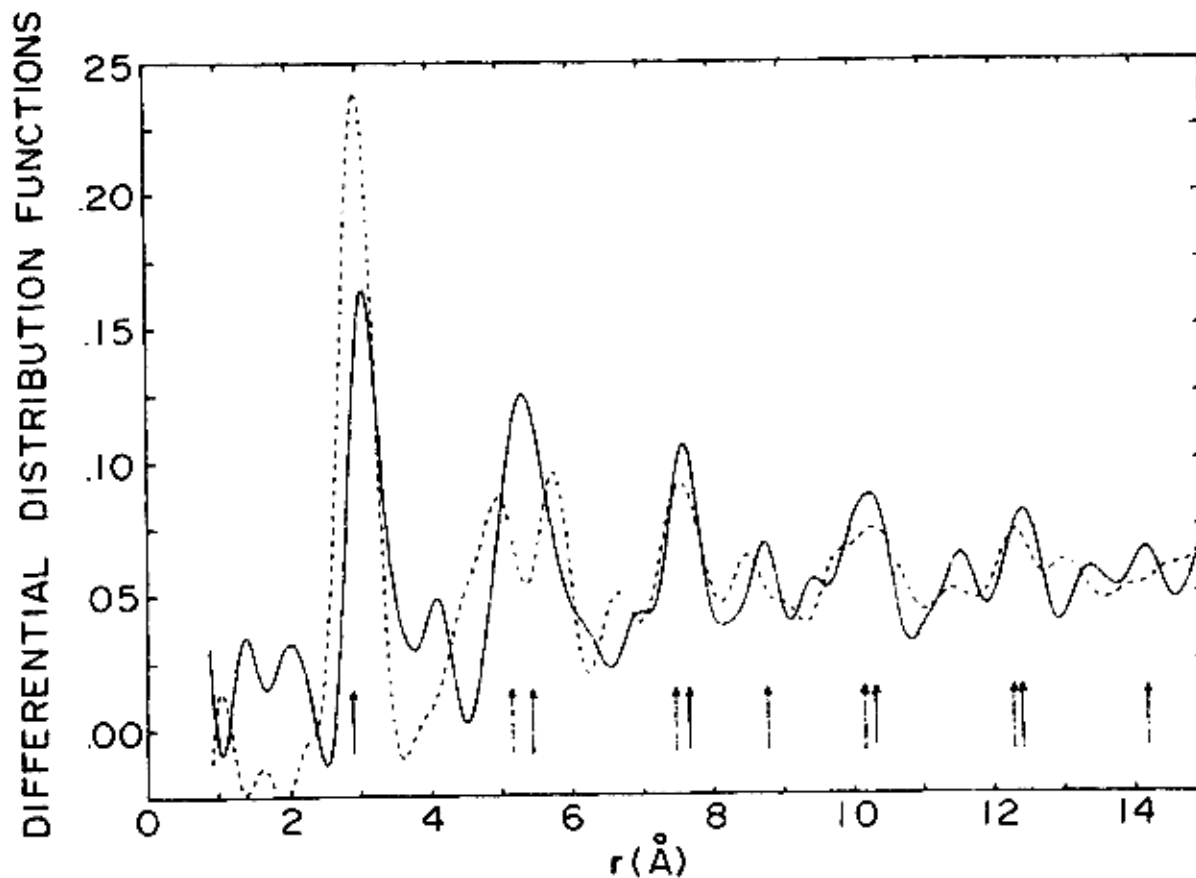
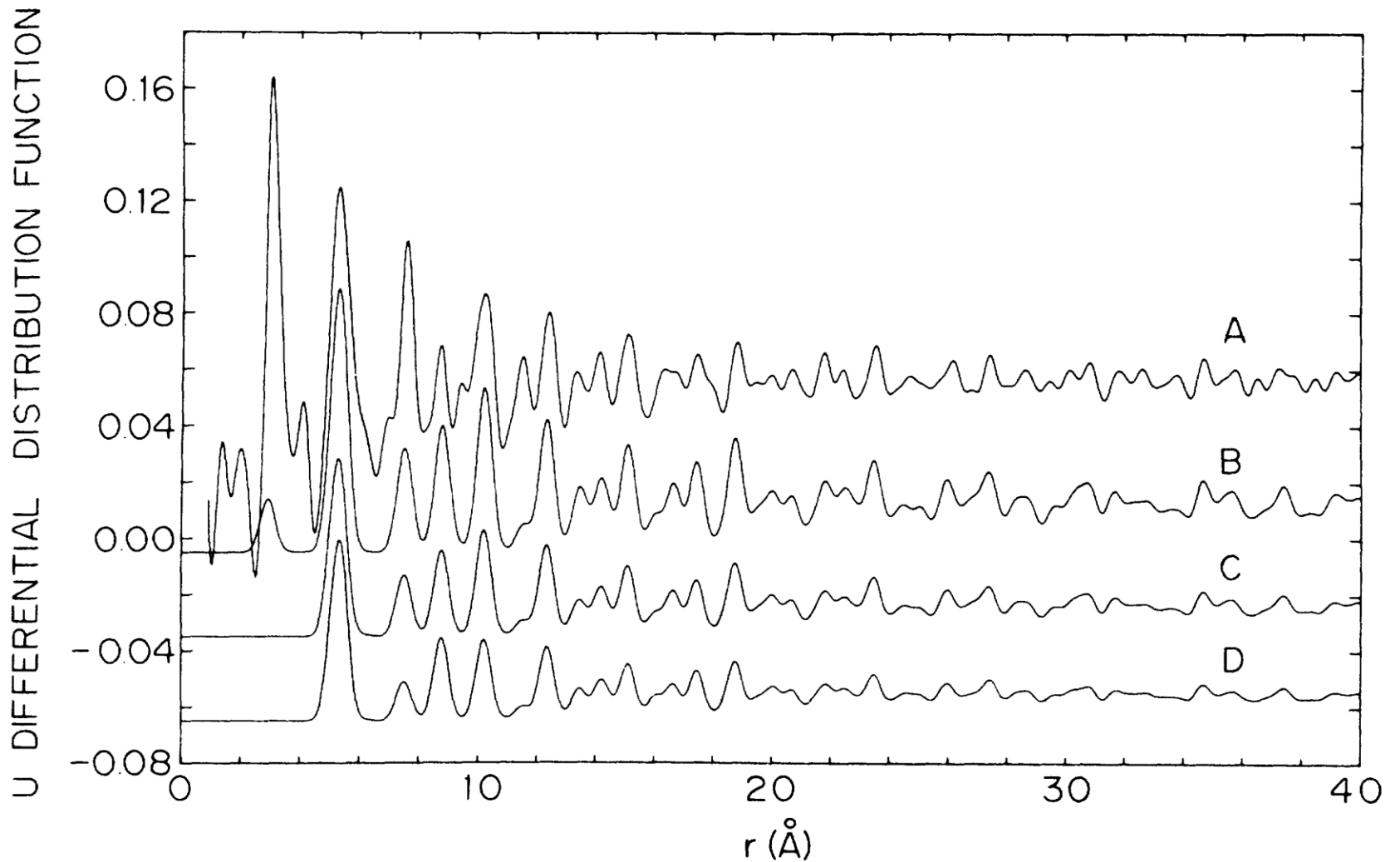


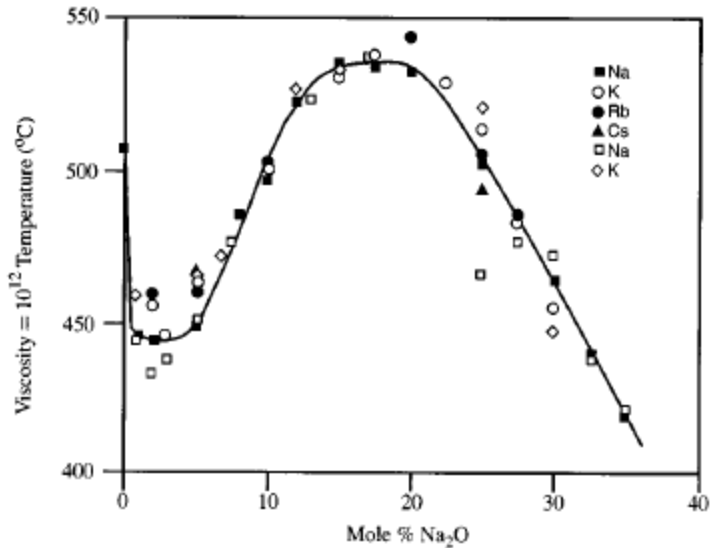
FIG. 3. Differential distribution functions of icosahedral $\text{Pd}_{58.8}\text{U}_{20.6}\text{Si}_{20.6}$, with uranium at the origin (full line), and with palladium at the origin (broken line).

S. Aur, D. Kofalt, Y. Waseda, T. Egami, R. Wang, H.S. Chen, and Boon-Keng Teo, *Solid St. Commun.* **48**, 111 (1983).

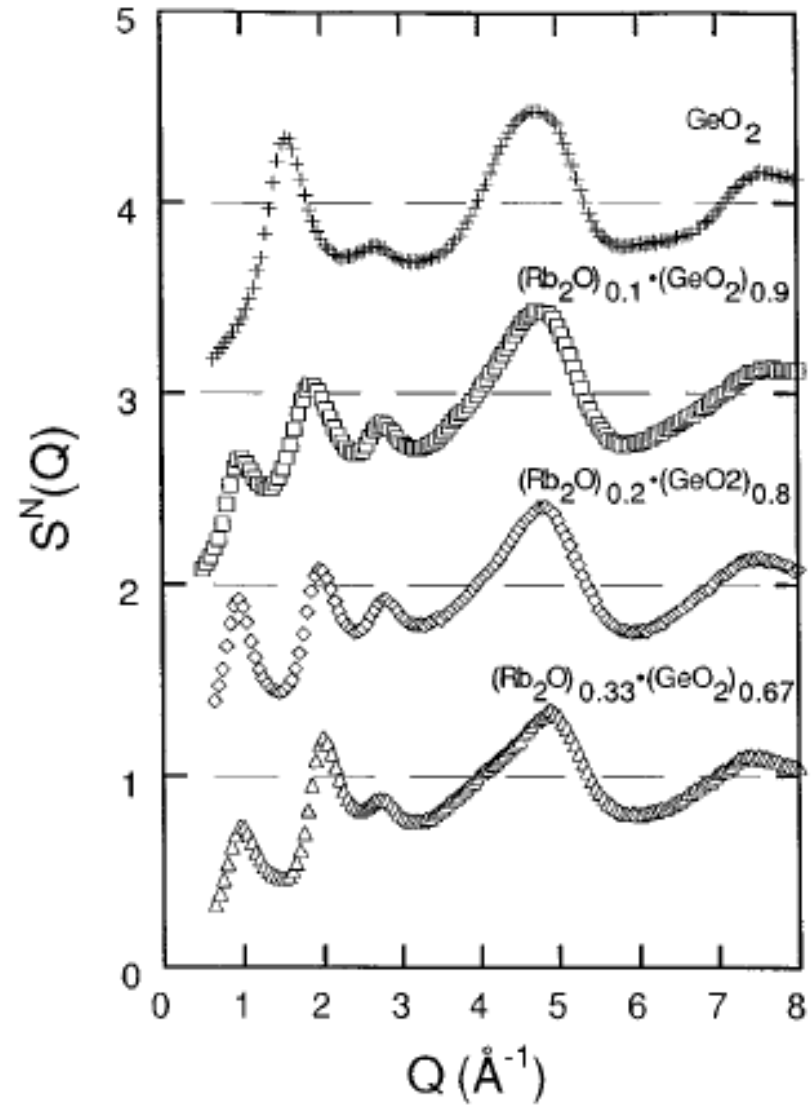


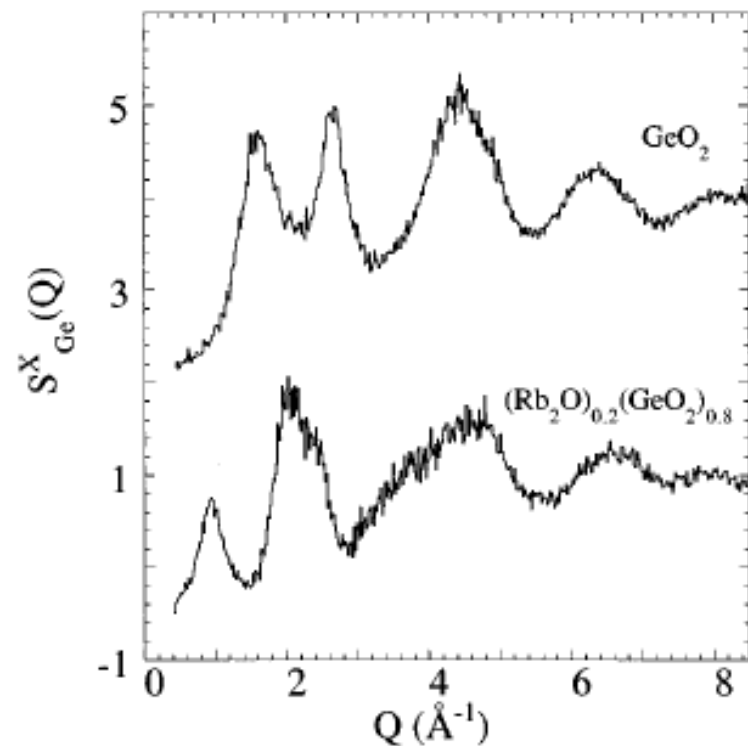
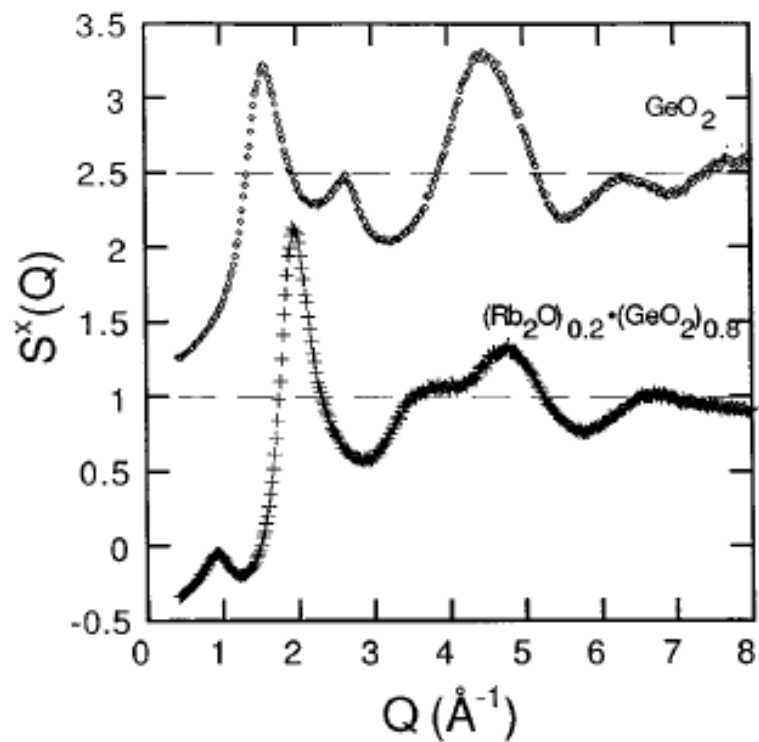
D.D. Kofalt, I.A. Morrison, T. Egami, S. Preische, S.J. Poon, and P.J. Steinhardt,
Phys. Rev. B **35**, 4489 (1987)

Structure of Rubidium Germanate



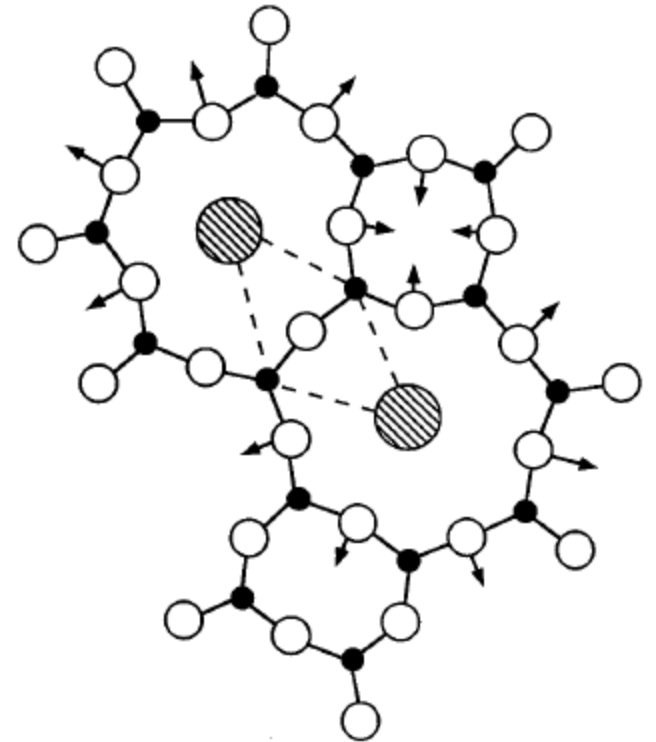
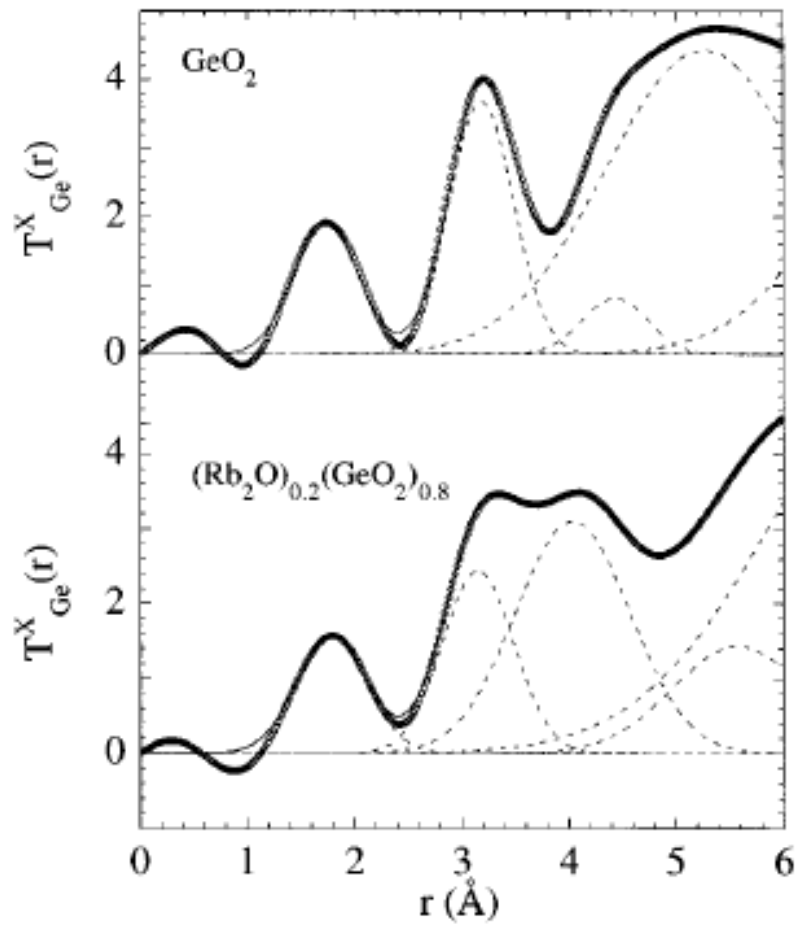
- Addition of Rb₂O to GeO₂ initially harden the glass, and softens it.





- Major change in the Ge DDF.

D.L. Price, A.J.G. Ellison, M.-L. Saboungi, R.-Z. Hu, T. Egami, and W.S. Howells, *Phys. Rev. B* **55**, 11249 (1997)



- Major change in the third NN of Ge.

Nano-Particles

- Au is inactive as bulk, but shows strong catalytic activity at nano-scale.
- AXS at the Au L-edge.

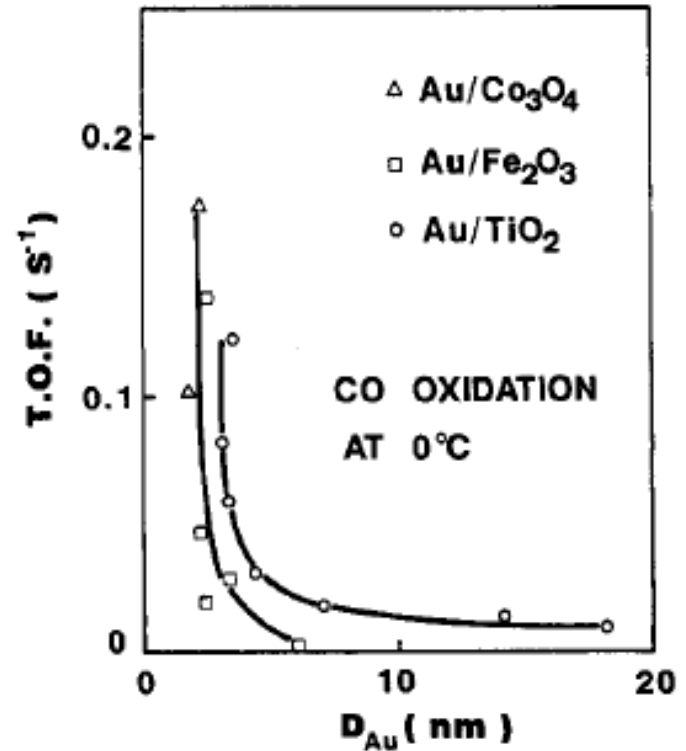
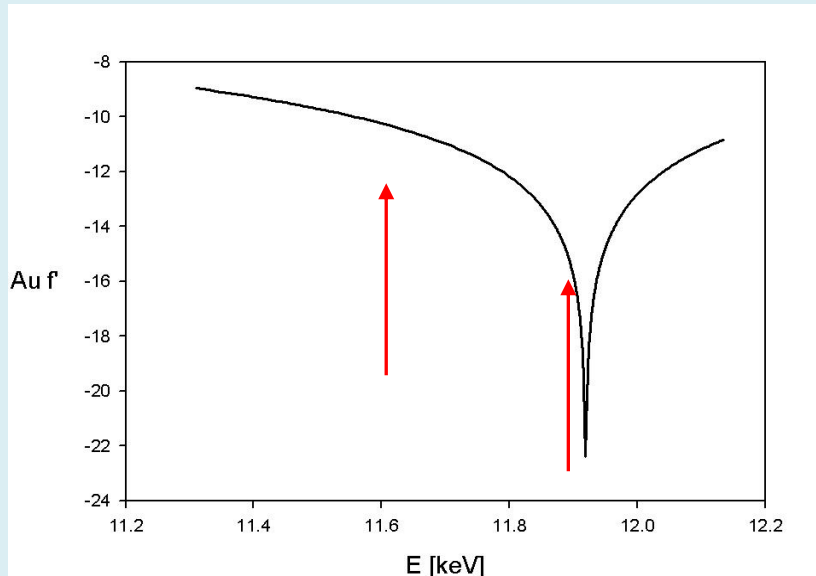
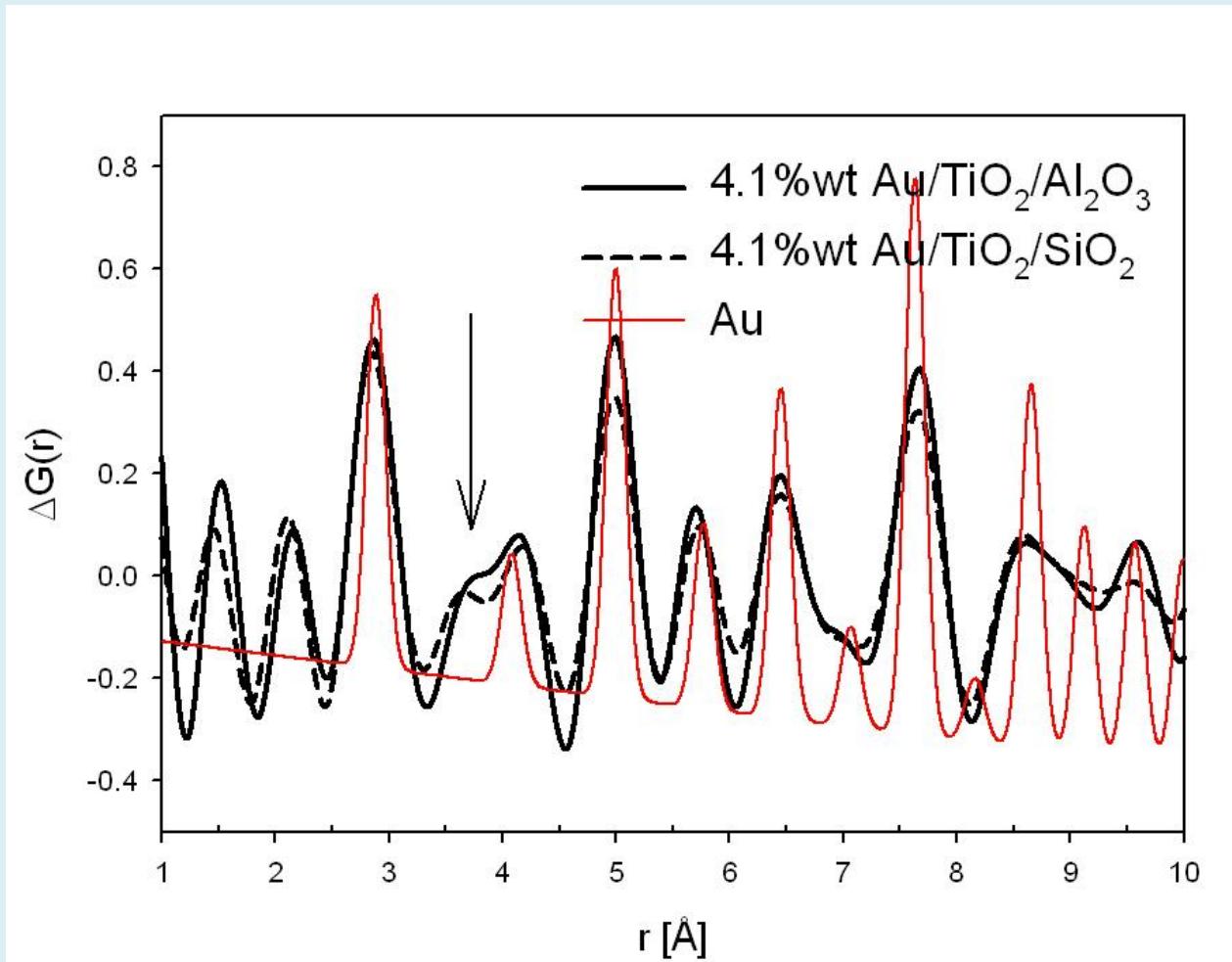
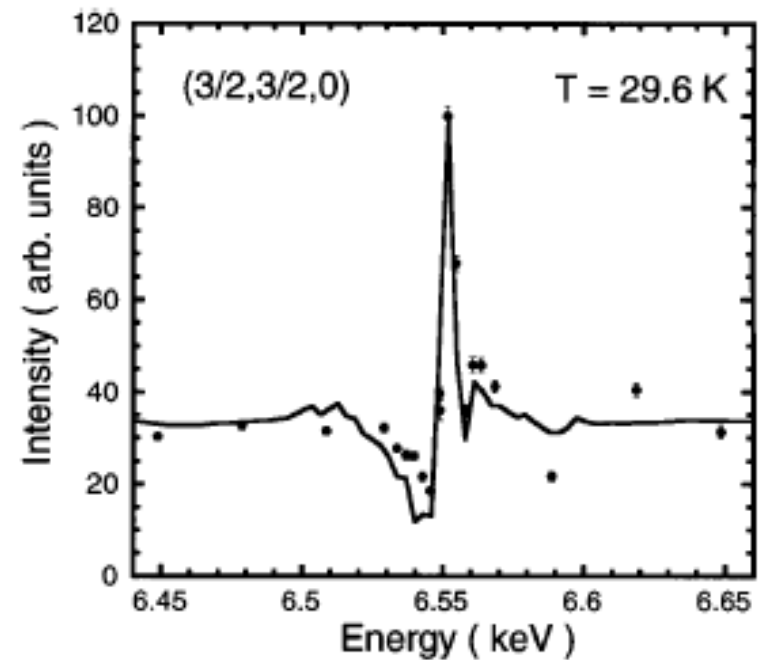
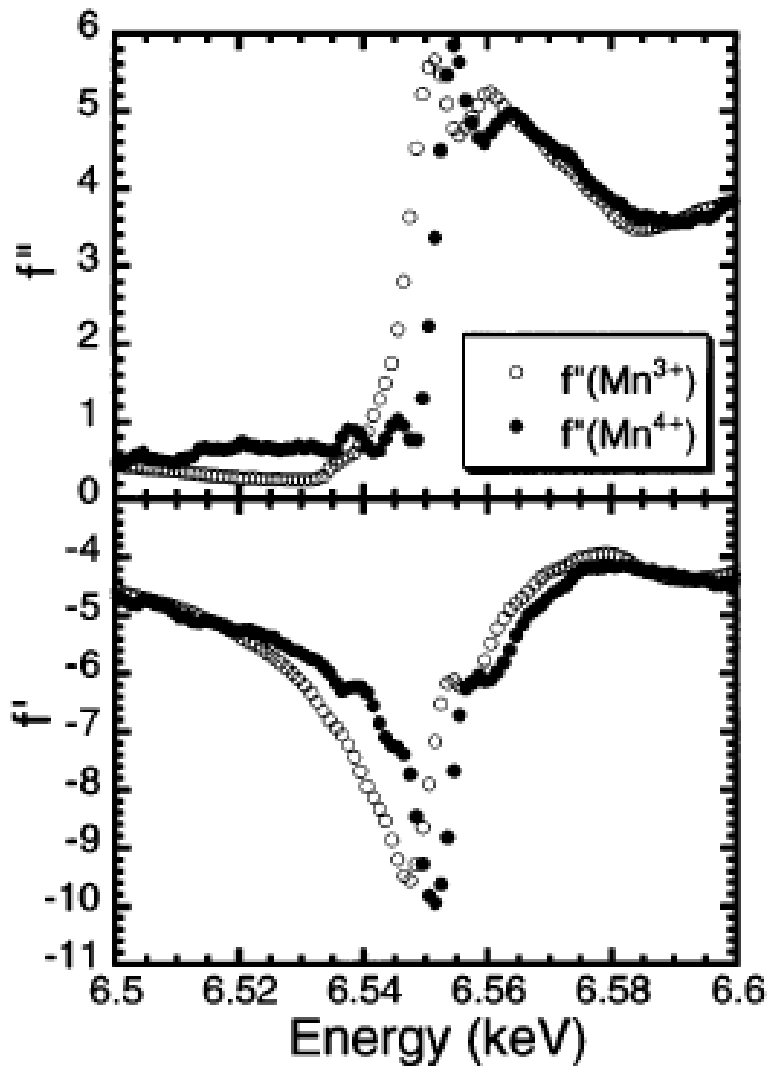


Fig. 4. Turnover frequencies based on surface exposed gold atoms as a function of the mean particle diameters of gold in CO oxidation at 0°C. Δ , Au/Co₃O₄; \square , Au/ α -Fe₂O₃; \circ , Au/TiO₂.



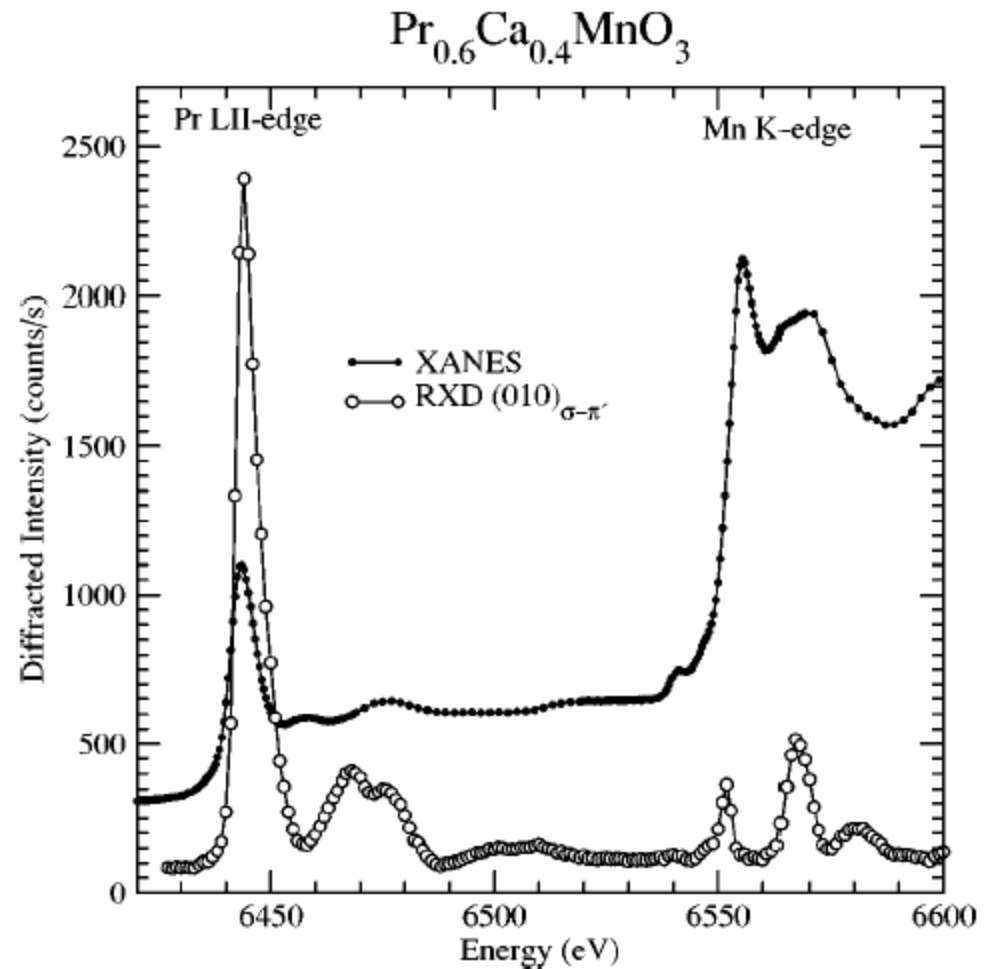
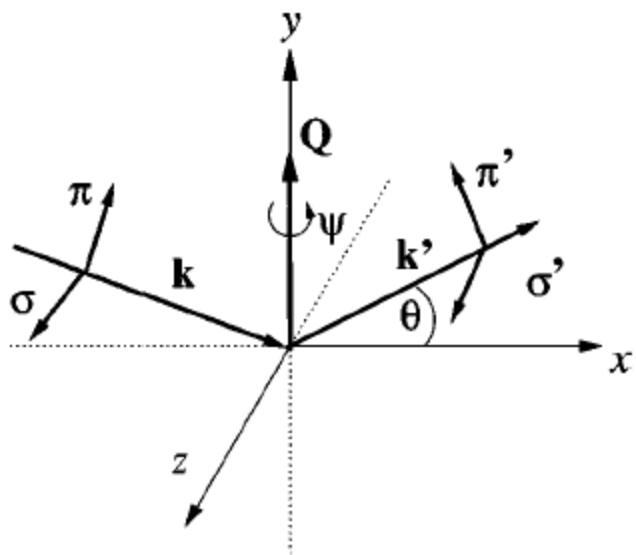
- Additional peak at 3.7 \AA .

Combining Spectroscopy with Diffraction



Resonant x-ray diffraction of the magnetoresistant perovskite $\text{Pr}_{0.6}\text{Ca}_{0.4}\text{MnO}_3$

S. Grenier,^{1,2} J. P. Hill,² Doon Gibbs,² K. J. Thomas,² M. v. Zimmermann,³ C. S. Nelson,⁴ V. Kiryukhin,¹ Y. Tokura,⁵
 Y. Tomioka,⁵ D. Casa,⁶ T. Gog,⁶ and C. Venkataraman⁶



Conclusions

- AXS is an excellent method to determine CSRO in glasses.
- It needs synchrotron radiation; if you have an access, it is a good method to consider.
- It gives information on medium-range order (cf. EXAFS).
- However, execution requires appropriate setup, sufficient statistics and careful data processing.
- You have to be careful with fluorescence and absorption correction.
- Not useful for light elements (consider neutron scattering with isotope substitution).